Reprint from

Topics in Applied Physics

Volume 9: **Laser Speckle and Related Phenomena**
Editor: J. C. Dainty
Second Enlarged Edition

Springer-Verlag
Berlin Heidelberg New York Tokyo

Laser Speckle and Related Phenomena

Editor: J. C. Dainty

Second Enlarged Edition

8. Recent Developments

J. C. DAINTY

With 6 Figures

Since this volume was first written in 1975, there have been many developments in the field of speckle. Some of these are summarized in this chapter. However, neither the topics nor the cited references give comprehensive coverage to all recent advances; the author has selected those subjects that, in his opinion, are the most interesting. A more complete account of recent work in speckle, is given in [8.1–6].

8.1 Statistical Properties

8.1.1 Gaussian Speckle

The type of speckle pattern discussed in Chapter 2 by J. W. Goodman is now usually referred to as "Gaussian speckle". This terminology is derived from the fact that, as a result of the rough surface approximation and the central limit theorem, the complex amplitude is a circular complex Gaussian process; as shown on p. 15, this results in a negative exponential probability density function for the intensity. Within the limits of the necessary conditions, the statistics of a Gaussian speckle pattern are independent of the nature of the scattering medium; in particular, the surface roughness σ_h does not influence the statistics provided that $\sigma_h \gtrsim \lambda$ and that a large number N of scatterers contribute to the intensity at any one point.

The existence and importance of Gaussian speckle has never been seriously questioned. The negative exponential distribution for the intensity and its independence of σ_h (for $\sigma_h \gtrsim \lambda$) have been confirmed experimentally many times. A reappraisal of the speckle effect [8.7], which claimed that Gaussian speckle could only be obtained using "media characterized by an inhomogeneity with an extent smaller than about $\lambda/100$" provoked a lively discussion [8.8, 9] but is not widely accepted as it contradicts all known experimental evidence. On the other hand, it must be emphasized that nearly all studies of speckle have assumed Kirchhoff diffraction for the interaction of the incident radiation

and the scatterer, and this is without doubt a very naive approach. Some recent studies [8.10] have shown that Kirchhoff theory is a reasonable approximation when $l \gtrsim 2\lambda$ and $\sigma_h/l \lesssim 0.05$, l being the correlation length of the surface.

Several new statistical properties of Gaussian speckle patterns have been evaluated recently. OCHOA and GOODMAN [8.11] have found the probability density function of ray directions in a speckle pattern. Speckle in multimode optical fibers has also been studied [8.12–14]; when the light loss due to radiative modes is small, a constraint of constant total power is introduced that is not present in the usual theory of integrated Gaussian speckle.

Let W represent the integrated intensity observed by a detector of area A_d in contact with the end of a step-index fiber of cross-sectional area A_f; then

$$W = \iint_{A_d} I(x, y) dx\, dy, \tag{8.1}$$

where $I(x, y)$ is the distribution of intensity across the end of the fiber core. Let M_T be the number of modes propagating in the fiber and let $0 \leqq \varrho \leqq 1$ be the ratio $\sqrt{A_d/A_f}$. By evaluating the conditional density of W given a total power constraint W_T, $p(W|W_T)$, GOODMAN and RAWSON [8.14] show that the signal-to-noise ratio $\bar{W}/\sigma_W$ is given by

$$\bar{W}/\sigma_W = \varrho \sqrt{\frac{M_T + 1}{1 - \varrho^2}}, \tag{8.2}$$

and not by the unconstrained value of $\varrho\sqrt{M_T}$. Their experimental measurements are compared to this result in Fig. 8.1.

Another interesting statistical property of Gaussian speckle is the probability density function of the spatial (or, for dynamic speckle, temporal) derivative of the intensity [8.15–17]. This is given by the Laplacian density,

$$p(\dot{I}) = \frac{1}{\sqrt{2\langle \dot{I}^2 \rangle}} \exp\left(\frac{-\sqrt{2}\dot{I}}{\langle \dot{I}^2 \rangle}\right), \tag{8.3}$$

where $\dot{I}$ denotes the derivative of I. Experiment and theory are compared in Fig. 8.2 [8.15]. If the intensity is first spatially integrated by a detector of finite area, and then differentiated, the probability density is given approximately by a K-distribution [8.17]. Indeed, the K-distributions are quite analogous to the gamma distributions in speckle theory; the gamma distributions describe the approximate probability density func-

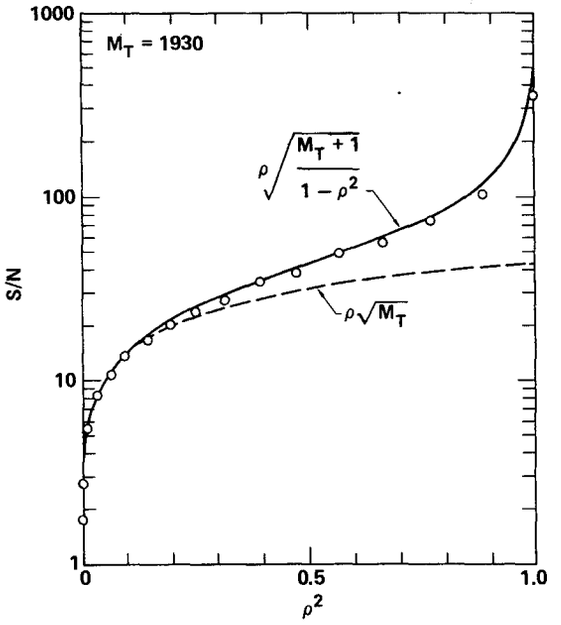

Fig. 8.1. Signal-to-noise ratio as a function of fractional detector area in the absence of a polarizer [8.14]. The dashed curve represents the square-root law of the conventional theory, the circles are experimental results and the solid curve represents the predictions of (8.2)

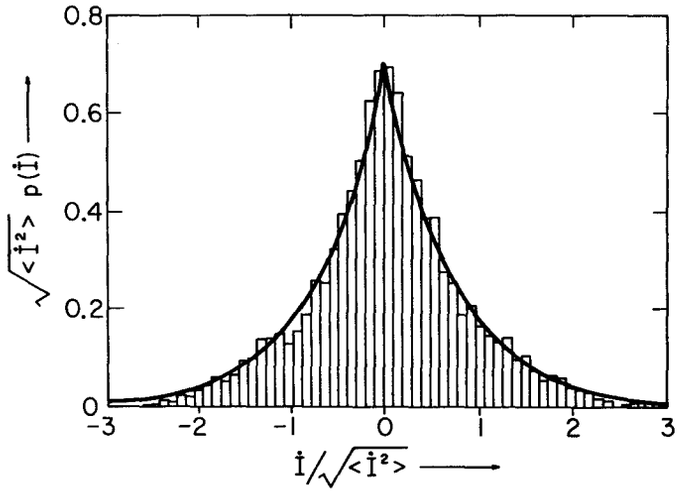

Fig. 8.2. Comparison of the measured histogram of the spatial derivative of the intensity (indicated by the bars) and the theoretical probability density $p(\dot{I})$ of (8.3) [8.15]

tion of integrated intensity in a speckle pattern (Sect. 2.6.2), whereas the K-distributions describe the approximate probability density function of integrated intensity in a differentiated speckle pattern.

If a large number of scatterers are present, but the path differences are not large compared to the wavelength, then the complex amplitude still has Gaussian statistics, but they are non-circular as was briefly discussed in Sect. 2.7.3. This so-called "partially developed" speckle ($\sigma_I/\langle I\rangle \leqq 1$) has been studied extensively because of its potential importance in the measurement of surface roughness (Sect. 8.3.1). UOZUMI and ASAKURA

[8.18] gave a complete description of partially developed speckle in the far-field, and OHTSUBO [8.19] has derived an expression for the probability density function of the derivative of partially developed speckle. The statistics of polychromatic Gaussian speckle are described in Chap. 3 and extended in [8.20, 21].

8.1.2 Speckle Reduction

Digital image processing techniques have recently been applied to the problem of reducing speckle noise in images [8.22–24]. These are almost always based on a multiplicative noise model of the form

$$I_{S+N} \propto I_S \cdot I_N . \tag{8.4}$$

where I_S, I_N, and I_{S+N} are the intensities for the signal, noise (speckle) and signal plus noise, respectively. Assumption (8.4) applies only when the signal is spatially uniform [8.25], which is rarely of any practical interest in speckle reduction. It does not apply when the signal contains details smaller than the speckle and an example of this is given in [8.25].

8.1.3 Speckle and Coherence Theory

The very close similarity between speckle and coherence theory was emphasized in Chap. 2. In speckle, we are interested in the statistical properties of *scattered* fields over an ensemble of *scatterers*, whereas in coherence theory the interest lies in *radiated* fields over an ensemble of *sources*. Thus, for example, the analysis in Sect. 2.5.1 leads to an amplitude autocorrelation function ("mutual intensity") of the speckle field that is the same as that predicted by the van Cittert-Zernike theorem of coherence theory, derived some 40 years earlier. On the other hand, the analysis in Sect. 2.7 dealing with speckle from diffusers of finite correlation area predates the recent work on quasi-homogeneous sources in coherence theory [8.26].

Several authors have discussed the relationship between speckle theory and coherence theory [8.27–29]. A circular Gaussian speckle pattern is, essentially, a static or "frozen" form of a thermal light field, and provides a convenient way of visualizing concepts in coherence (for example, speckle area ≡ coherence area). However, the source problem (coherence) and scattering problem (speckle) are physically quite different and it is difficult to see the usefulness of stretching the analogy further, especially for non-Gaussian speckle patterns or non-thermal sources in coherence theory.

If the speckle is dynamic (Sect. 8.2), then the analogy becomes more complicated. For example, it is well-known that the spatial correlation of the instantaneous scattered field from a rotating diffuser (or "quasi-thermal source" [8.30]) is given by the van Cittert-Zernike theorem of coherence theory. However, it has been shown [8.31] that the spatial correlation of the time-integrated speckle field is *not* in general given by the van Cittert-Zernike theorem, so that some care is necessary when simulating states of partial coherence with speckle patterns. Another interesting area of comparison is the detection of phase gratings "hidden" by diffusers [8.32, 33].

8.1.4 Non-Gaussian Speckle

The statistics of circular Gaussian speckle tell us little about the scattering medium, apart from the fact that a large number N of independent scattering areas are present and that the optical path fluctuations due to the medium are greater than a wavelength. On the other hand, if only a few independent scattering areas are present, then the speckle statistics do contain information about the scattering medium, although extraction of this information may not be straightforward. Such "small-N" speckle usually (but not necessarily) has non-Gaussian statistics for the complex amplitude, and hence the probability density function of intensity is usually not negative exponential.

JAKEMAN, PUSEY and co-workers [8.34–39] have made the most significant contribution to the theory of small-N or non-Gaussian speckle in the rough surface limit ($\sigma_h \gtrsim \lambda$); work in the smooth surface limit is summarized in [8.40]. For scattering from surfaces, two models have been used. The simplest is the facet model, in which the complex amplitude in the observation plane is expressed as the sum of N independent contributions:

$$A = \sum_{j=1}^{N} a_j \exp(\mathrm{i}\phi_j), \tag{8.5}$$

where the ϕ_j are uniformly distributed between $-\pi$ and π and the scattering amplitudes a_j have a probability density of $p(a_j)$. This is the classic finite random walk problem in two dimensions; if the ϕ_j are independent of the a_j, then Lord Rayleigh [8.41] showed that the probability density function of the intensity is given by

$$p(I) = \tfrac{1}{2} \int_0^\infty \mathrm{J}_0(u\sqrt{I})u \langle \mathrm{J}_0(ua) \rangle^N du, \tag{8.6}$$

where J_0 is the zero order Bessel function, and $\langle\ \rangle$ denotes an average over the ensemble of scattering amplitudes.

Equation (8.6) cannot be reduced further without some assumption being made about the statistical properties of the a_j. However, the moments of intensity can be found, for example

$$\left.\begin{aligned} &\langle I\rangle = N\langle a^2\rangle \\ &\langle I^2\rangle/\langle I\rangle^2 = 2(1-N^{-1}) + N^{-1}\frac{\langle a^4\rangle}{\langle a^2\rangle^2} \end{aligned}\right\} \tag{8.7}$$

Clearly, the normalized second moment tends to the Gaussian value of 2 as $N\to\infty$.[1] When N is finite there is typically an excess fluctuation proportional to N^{-1} (i.e., inversely proportional to the illuminated surface area); the magnitude of this excess fluctuation depends on the statistics of the scattering amplitudes.

Although the above model is an exact one for scattering by discrete particles, it is inadequate for scattering from rough surfaces, especially when the area of illumination is of the same order of magnitude as the correlation area of the surface. A more satisfactory model (but still an approximation) is based on Kirchhoff's (scalar) diffraction theory. The problem in this case is that although integral formulae for the moments of intensity can be written down, they can only be evaluated for surfaces with a Gaussian probability density of surface height, certain special forms of spatial correlation function and for a Gaussian illumination spot; even then, only the first and second moments of intensity can be written in closed form.

Experimental measurements of the second moment of intensity for small-N or non-Gaussian speckle from ground glass diffusers [8.42] do not agree with the above theory for single-scale surfaces; however, recent measurements using specially prepared single-scale surfaces [8.43] give excellent agreement, as shown in Fig. 8.3. It is believed that measurements of speckle contrast obtained using ground-glass surfaces are more likely to agree with the theory of scattering by fractal or sub-fractal surfaces [8.39, 44]. The wavelength dependence of non-Gaussian speckle has also been studied [8.45].

The phenomenon of random caustics is closely related to small-N speckle [8.46, 47]. For small wavelengths λ, the intensity moments $\langle I^n\rangle/\langle I\rangle^n$ are inversely proportional to λ^{ν_n}, where ν_n are called the twinkling exponents; measurements of ν_n from refraction through an irregularly rippling water surface at two wavelengths have recently been reported [8.48].

---

[1] It is assumed than N is not also a random variable.

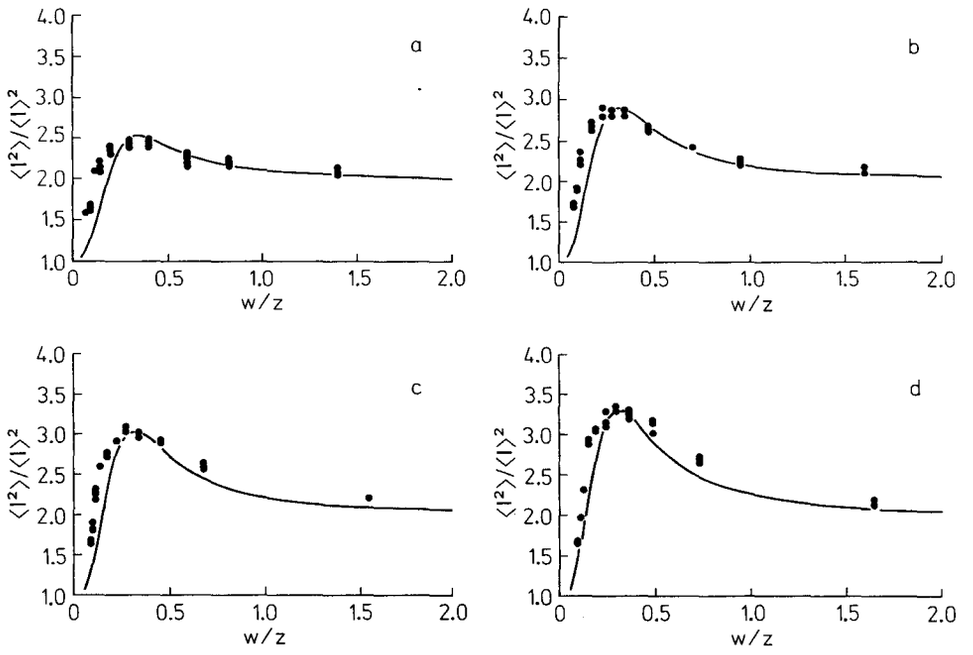

Fig. 8.3a–d. Normalized second moment of intensity as a function of the "number of scatterers" $N \equiv (W/z)^2$ for four diffusers (a)–(d); the experimental results agree well with the theoretical predictions (*solid curves*) [8.43]

Another interesting situation in which non-Gaussian speckle can arise is in the case of doubly scattered light. This occurs when speckle patterns propagate through the atmosphere [8.49] or from a cascade of two diffusers ("speckled speckle") [8.50–52]. Consider the case in which a diffuser of a certain area is illuminated by a Gaussian speckle pattern containing M speckle correlation areas; it is assumed that, considering the illumination as a deterministic quantity, the diffuser would give a Gaussian speckle pattern. However, viewing the illumination as a stochastic process, it can be shown [8.52] that the probability density function of intensity is of the form

$$p(I) = \frac{2}{\Gamma(M)} \frac{1}{\beta} \left(\frac{I}{\beta}\right)^{(M-1)/2} \mathrm{K}_{M-1}\left(2\sqrt{\frac{I}{\beta}}\right). \tag{8.8}$$

where $\beta = \langle I\rangle/M$, $\mathrm{K}_\mu(x)$ is the modified Bessel function of order μ and argument x, and $\Gamma(M)$ is the gamma function. The normalized variance of the intensity in this case is

$$\sigma_I^2/\langle I\rangle^2 = 1 + \frac{2}{M}. \tag{8.9}$$

Thus if the speckle area in the illuminating beam is very much larger than the area of the diffuser (i.e., $M=1$), the normalized variance is 3, compared to the Gaussian value of 1 (which is obtained in the limit $M\to\infty$). The spatial correlation function of doubly scattered light is also evaluated in [8.52].

8.2 Dynamic Speckle

If the scattering medium changes with time, the speckle pattern also evolves and the phenomenon is known as "dynamic speckle". Clearly, information about the change in the medium (e.g., its velocity) is present in the dynamic speckle pattern, although extraction of this information is only possible in certain special cases.

Two different temporal changes can arise in a speckle pattern depending on the nature of the change in the scattering medium, the illumination geometry and the viewing situation (far-field or image plane). In certain cases, the speckle pattern moves as a whole without any other significant change in the pattern—this is referred to as a *translating* speckle pattern and typically occurs in the image of a diffuse object that is moving perpendicular to the line-of-sight. In other cases, the individual speckles evolve continuously, disappearing and reappearing without any appreciable displacement of their positions—this is referred to as a *boiling* speckle pattern and typically occurs in the far-field of a moving diffuse object. Most dynamic speckle patterns contains both boiling and translating elements.

If we restrict our attention to Gaussian speckle patterns, then the complete statistical properties of dynamic speckle are described by the space-time correlation function,

$$C_A(\boldsymbol{x}_1, \boldsymbol{x}_2; t_1, t_2) \equiv \langle A(\boldsymbol{x}_1, t_1) A^*(\boldsymbol{x}_2, t_2) \rangle . \tag{8.10}$$

In many practical situations, the speckle pattern is effectively spatially and temporally stationary (in the statistical sense) and the correlation of intensity fluctuation is measured:

$$C_{\Delta I}(\Delta \boldsymbol{x}, \Delta t) \equiv |C_A(\Delta \boldsymbol{x}, \Delta t)|^2 . \tag{8.11}$$

The spatio-temporal cross-correlation of dynamic speckle from a rigidly translating object was first studied by ANISIMOV et al. [8.53] and subsequently by ASAKURA [8.54–56] and O'DONNELL [8.57]. A complete discussion of the form of the spatio-temporal correlation function is

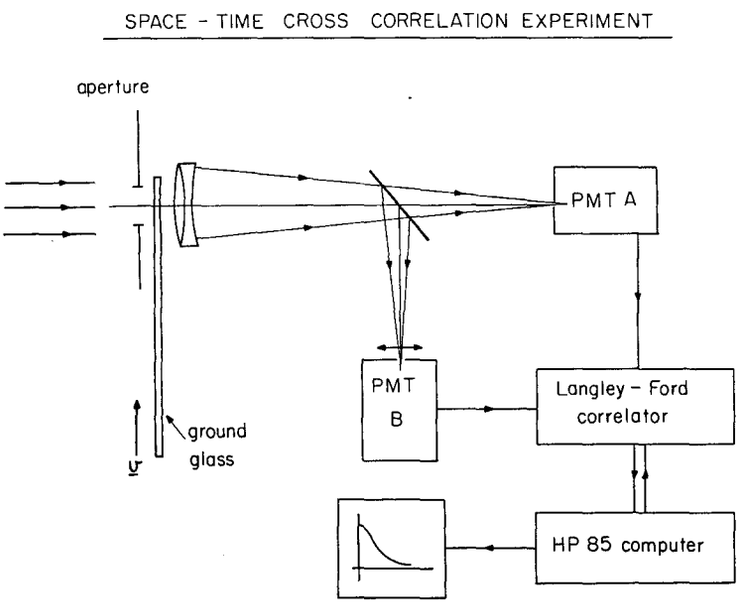

Fig. 8.4. Experimental apparatus used in measuring spacetime correlations [8.57]. Photomultiplier B is mounted on a translator that introduces a known $(\Delta x, \Delta y)$ between the two detectors and the temporal correlation of the two detector signals is measured with a photon correlator

beyond the scope of this article; however, to illustrate the subtle way in which this can code information about an optical system, we shall discuss the spatio-temporal correlation function of dynamic speckle formed in the focal region of a lens with a moving diffuser placed in front of it [8.57].

Consider the experiment shown in Fig. 8.4; a diffuser moves linearly at velocity v along the ξ axis of a (ξ, η) rectangular coordinate plane in which a lens is placed. If the diffuser has a sufficiently small correlation area, the speckle pattern observed in the region of the focal plane (x, y) is effectively spatially stationary. Two photomultipliers are placed $(\Delta x, \Delta y)$ apart and the normalized temporal cross-correlation of intensity fluctuation,

$$C'(\Delta x, \Delta y, \Delta t) = \frac{\langle \Delta I(x, y, t) \Delta I(x + \Delta x, y + \Delta y, t + \Delta t) \rangle}{\langle I \rangle^2},$$

is measured using standard methods. By repeating this experiment for many separations $(\Delta x, \Delta y)$, the complete spatio-temporal correlation function can be measured.

Figure 8.5a–d summarizes the experimental results for a square lens pupil of side a. In each case temporal cross-correlation curves are plotted

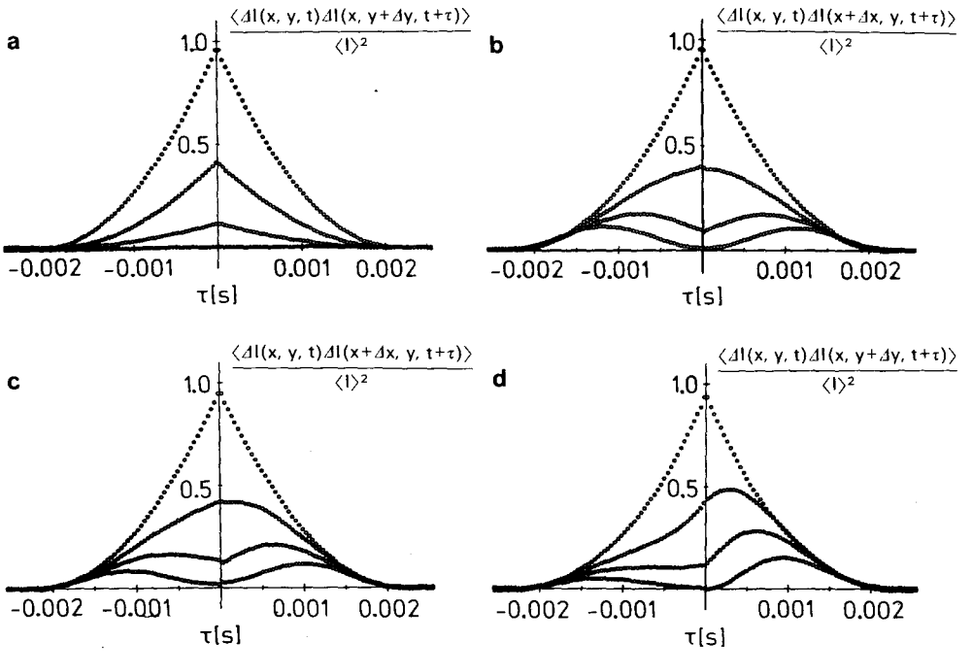

Fig. 8.5a–d. Space-time correlation functions measured in region of the focal plane [8.57]. [(a) detectors displaced 0, 0.5, 0.75, and 1.0 speckle radii along y (top to bottom of figure). (b) detectors displaced by 0, 0.5, 0.75, and 1.0 speckle radii along x. (c) as (b), but a defocus of 0.025 waves. (d) as (b), but a defocus of 0.09 waves]

for detector separations of 0, 0.5, 0.75, and 1.0 speckle radii, where a speckle radius is equal to $\lambda f/a$; in Fig. 8.5a the detectors are separated along Δy (perpendicular to the diffuser motion) and in Fig. 8.5b–d they are along Δx (parallel to the diffuser motion).

Figure 8.5a and b show the spatio-temporal behaviour of the speckle pattern in the focal plane for spatial separations perpendicular and parallel, respectively, to the diffuser motion. In both cases the $(\Delta x, \Delta y) = (0,0)$ curve is the temporal autocorrelation function of the intensity fluctuations, and a straightforward analysis shows that this equals the squared modulus of the *optical transfer function* of the lens:

$$C'(0,0,\Delta t) = \left| \frac{\int\int_{-\infty}^{\infty} P(\xi,\eta)P^*(\xi+v\Delta t,\eta)d\xi\,d\eta}{\int\int_{-\infty}^{\infty} |P(\xi,\eta)|^2 d\xi\,d\eta} \right|^2, \tag{8.12}$$

where $P(\xi,\eta)$ is the pupil function of the lens. Equation (8.12) forms the basis of a simple method of measuring the modulation transfer function of an optical system.

A further investigation of Fig. 8.5a and b shows that the spatio-temporal correlation is quite different for detector spacings perpendicular to the diffuser motion, Fig. 8.5a, and parallel to the motion, Fig. 8.5b. The constancy of the shapes of the curves in the former case means that $C'(\Delta x, \Delta y, \Delta t)$ can be factorized as

$$C'(\Delta x, \Delta y, \Delta t) = C'_1(\Delta x, \Delta t) C'_2(\Delta y),$$

but the variation of curve shapes in Fig. 8.5b means that no further factorization is possible. In the language of coherence theory, a dynamic speckle pattern is not, in general, cross-spectrally pure [8.58]. In certain special cases, for example a Gaussian pupil function, complete factorization is possible.

Consider now the sequence of results shown in Fig. 8.5b–d, for defocus values of 0, 0.025, and 0.09 waves (measured at the edge of the pupil). For no defocus, the $\Delta x = 1$ speckle radius curves shows a double peaked structure, indicating simultaneous speckle motion both parallel and antiparallel to the diffuser motion. As the defocus increases from zero, the speckle motion tends to be in one direction in accordance with simple geometrical optics—the cross-correlation curves are strongly skewed in one direction. It is surprising that defocus values as small as 1/40th of a wave can be detected from the spatio-temporal data and this could form the basis of a method of automatic focussing [8.59].

The above experimental data is in excellent agreement with theory [8.57]. The spatio-temporal behaviour of dynamic speckle does depend on the detailed geometry of the experiment and the nature of the object's motion, and other cases were reviewed in [8.55]. One particularly interesting situation is the spatio-temporal behaviour of speckle produced by rotating diffuse objects such as spheres [8.60–63].

Although many techniques of object velocity determination using dynamic speckle are based on correlation measurements, in some situations a simple measurement of the zero-crossing rate of a differentiated speckle pattern may be adequate [8.64]. The exact solution of the zero-crossing rate in differentiated speckle patterns has been given by OHTSUBO [8.65].

8.3 Speckle Metrology

Many of the recent developments in speckle metrology were described in the book *Speckle Metrology* [8.4] and in the review by ENNOS [8.66].

8.3.1 Measurement of Surface Roughness

Speckle patterns can be used in several different ways to estimate the statistics of the height distribution of a rough surface [8.67, 68], although a general method of solving the inverse scattering problem has not yet been found. As stressed earlier this chapter and in Chap. 2, the statistics of monochromatic, circular, Gaussian speckle patterns are independent of surface properties, provided that certain conditions are met. Monochromatic circular Gaussian speckle patterns can still, however, be used to measure surface roughness by correlating two such patterns obtained by illuminating the surface from two different directions [8.69]; in this case one is using the speckle patterns as deterministic carriers of information and not contradicting the statement that the *statistics* are independent of surface roughness.

Three methods of measuring surface roughness using the statistical properties of speckle have been suggested: (a) for smooth surfaces, $\sigma_h \lesssim \lambda/4$, monochromatic non-circular Gaussian speckle [8.70], (b) for rough surfaces, $\sigma_h \gtrsim \lambda/4$, monochromatic small-$N$ or non-Gaussian speckle [8.42] and (c) for rough surfaces, $\sigma_h \gtrsim \lambda/4$, polychromatic speckle (as described in Chap. 3).

An example of the use of the contrast of non-circular Gaussian speckle in the measurement of surface roughness is shown in Fig. 8.6 [8.42], for observation in the far-field and image planes. The theory predicts quite different results for these two cases and the agreement between theory and experiment is good. This method is practical over a range of roughness $\lambda/40 \lesssim \sigma_h \lesssim \lambda/4$, for reflective surfaces at normal incidence.

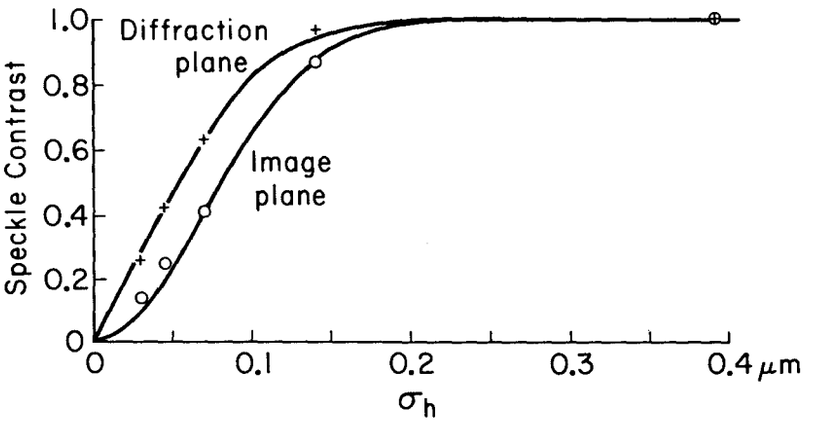

Fig. 8.6. The variation of speckle contrast with the rms surface roughness in the image and diffraction planes [8.42]

The statistics of small-N (non-Gaussian) speckle have been discussed in Sect. 8.1.4. Whilst these offer the possibility of measuring surfaces whose height fluctuation is greater than $\lambda/4$, there is a major problem due to the fact that the speckle contrast is also very sensitive to the form of the spatial autocorrelation function of the surface. At present there is no satisfactory method based on non-Gaussian speckle, at least for rough surfaces. Many of the studies of the feasibility of measuring surface roughness using speckle have relied upon computer simulations of speckle [8.71–74].

8.3.2 Speckle-Shearing Interferometry

An important instrumental improvement for providing information on the change of surface slope (Sect. 6.4.4) is the speckle camera of HUNG [8.75] which uses a thin glass wedge covering half the lens aperture to give the shear. This design of camera has proved to be the most effective in generating an appreciable number of high contrast slope change contour fringes by optical filtering of a recorded double exposure negative; the attainment of high contrast fringes is at the expense of limiting the measurement to one azimuth direction only.

The measurement of surface tilt by defocused speckle photography (Sect. 6.6.2) is closely related to speckle shearing interferometry, but it has the distinction of using the full aperture of the lens and can therefore give information on slope changes in any azimuth direction. GREGORY [8.76] has exploited this technique to detect faults in mechanical structures and indicates the high sensitivity of the method. However, his method of analysis uses the full field fringe patterns generated by spatial filtering which makes for complication in the interpretation.

If one of the shearing methods is used to measure slope change along a line in the surface, and values are integrated with respect to distance along the line, then the out-of-plane displacement can be derived. ENNOS and VIRDEE [8.77] measured the dilation of a hydraulic cylinder in situ in this way, and compared the results with holographic interferometry of the same subject; in this case, speckle and holographic interferometry have comparable sensitivities [8.78] but the speckle method is subject to error due to instrumental causes.

8.3.3 Scattered Light Speckle Photography

Measurement of the three-dimensional displacement of points within a translucent scattering medium can be carried out by directing a narrow beam of laser light through the body of the structure and photographing

the scattered light with two cameras mounted orthogonally to the beam. Double exposure photographs yield δx and δy for points along the beam [8.79, 80]. Higher sensitivity to internal displacement can be achieved by returning the laser beam along its path with a mirror and then obtaining speckle correlation fringes by the method described in Sect. 6.4.3.

A similar technique was developed by DUDDERAR and SIMKINS [8.81] for measuring velocity distributions within a fluid passing down a tube. A double pulsed laser beam is directed through the seeded medium and the speckle pattern from it photographed from the side.

8.3.4 Speckle Photography

The primary aim of the speckle technique is to provide a simple method of measuring surface displacement and hence the strain field. However, the precision of measurement is dependent upon the quality of the imaging system and considerable errors in strain values can result with standard lenses, due to a combination of tilting of the surface and lens aberrations [8.82, 83]. STETSON [8.84] has considered the general problem of measuring the complete displacement vector field and shows that it should be possible to do this by recording two speckle photographs in different focus planes. Lens aberrations, especially over a large angular fields, still produce significant strain errors.

The problem of compensating for large rigid body movement can be overcome by recording two separate speckle photographs and comparing them by a "sandwich" technique [8.85, 86]. Another technique consists of recording Lippmann type holograms by "contact printing" the photographic plate on to the surface with a broad laser beam. A reflection hologram is formed which when interrogated by a laser probe gives Young's type fringes due to the in-plane displacement.

Considerable effort has gone into automatic methods for the read-out of the displacement vectors from double exposure speckle photographs [8.88–90] by the point-by-point measurement of the Young's fringe separation and orientation. The aim of all the methods is to collect the maximum amount of information from the fringes to ensure high accuracy in computing the fringe spacing using the fast Fourier transform.

Applications

Novel applications up to 1978 were reviewed in [8.4]; examples include measurements on pressure vessels, a radar dish and the detection of cracks in an aircraft wing. Cracks in concrete have been detected using

focused image speckle photography by de BACKER [8.91], and FELSKE and HAPPE [8.92] have measured distortion of engine bearings by the same technique. The shake of a camera as a result of shutter movement has been investigated [8.93, 94] by analysis of speckle photographs and the motion path of the smeared image measured. Laser speckle photography also initiated the development of white light "speckle" techniques which use artificial speckles and require high definition camera lenses [8.95, 96].

8.3.5 Electronic Speckle Pattern Interferometry (ESPI)

Considerable development work has been carried out by Butters in [Ref. 8.4, Chap. 6] to improve ESPI. The principal advances are the use of a pulsed laser for vibration studies [8.97], the development for two-wavelength methods for optical contouring of simple shapes and two-wavelength methods for comparison of engineering components with a master (in this case it is necessary to use a specularly polished master surface or the image of it reconstructed from a hologram).

Design parameters for ESPI were discussed by JONES and WYKES [8.98] who also considered decorrelation effects [8.99, 100]. A commercial electronic speckle pattern interferometer is marketed by Vinten Ltd. (UK), who have developed a vibration measuring system for non-destructive testing in which the reference beam can be modulated by a vibrating mirror and the mode patterns displayed on a video display [8.101]. Very high sensitivity of vibration amplitude has been achieved by LOKBERG [8.102] who has directly observed the vibration of the human eardrum [8.103].

Acknowledgements. I am grateful to A. E. Ennos for providing notes for Sect. 8.3.2–5.

References

8.1 Special issue of J. Opt. Soc. Am. **66** (November 1976)
8.2 Proceedings of conference on Applications of Speckle Phenomena, Proc. SPIE **243** (1980)
8.3 Special issues of Opt. Engrg. **21**, Pts. 3 and 4 (1982)
8.4 R. K. Erf (ed.): *Speckle Metrology* (Academic, New York 1978)
8.5 M. Françon: *Laser Speckle and Applications in Optics* (Academic, New York 1979)
8.6 R. Jones, C. Wykes: *Holographic and Speckle Interferometry* (University Press, Cambridge 1983)
8.7 G. Ross, M. A. Fiddy: Opt. Acta **25**, 205 (1978)
8.8 H. M. Pedersen: Opt. Acta **25**, 1013 (1978); *see also* **25**, 1015 (1978), **26**, 149 and 153 (1979)
8.9 J. C. Dainty: Proc. SPIE **243**, 2 (1980)
8.10 M. Nieto-Vesperinas, N. Garcia: Opt. Acta **28**, 1651 (1981)

8.11 E. Ochoa, J. W. Goodman: J. Opt. Soc. Am. **73**, 943 (1983)
8.12 B. Daino, G. de Marchis, S. Piazzolla: Electron. Lett. **15**, 755 (1979)
8.13 E. G. Rawson, J. W. Goodman, R. E. Norton: Opt. Lett. **5**, 357 (1980)
8.14 J. W. Goodman, E. G. Rawson: Opt. Lett. **6**, 324 (1981)
8.15 K. J. Ebeling: Opt. Acta **26**, 1345 (1979)
8.16 K. J. Ebeling: Opt. Acta **26**, 1505 (1979)
8.17 K. J. Ebeling: Opt. Commun. **35**, 323 (1980)
8.18 J. Uozumi, T. Asakura: Appl. Opt. **20**, 1454 (1981)
8.19 J. Ohtsubo: J. Opt. Soc. Am. **72**, 1249 (1982)
8.20 C. T. Stansberg: Opt. Commun. **23**, 303 (1977)
8.21 Y. Tomita, K. Nakagawa, T. Asakura: Appl. Opt. **19**, 3211 (1980)
8.22 A. K. Jain, C. R. Christensen: Proc. SPIE **243**, 46 (1980)
8.23 J. S. Lee: Comp. Graph. Image Proc. **17**, 24 (1981)
8.24 J. S. Lim, H. Nawab: Opt. Engrg. **20**, 472 (1981)
8.25 M. Tur, K. C. Chin, J. W. Goodman: Appl. Opt. **21**, 1157 (1982)
8.26 H. Carter, E. Wolf: J. Opt. Soc. Am. **67**, 785 (1977)
8.27 J. W. Goodman: Proc. SPIE **194**, 86 (1979)
8.28 J. C. Leader: Opt. Engrg. **19**, 593 (1980)
8.29 H. M. Pedersen: Opt. Acta **29**, 105 (1982)
8.30 W. Martienssen, E. Spiller: Am. J. Phys. **32**, 919 (1964)
8.31 T. Gonsiorowski, J. C. Dainty: J. Opt. Soc. Am. **73**, 234 (1983)
8.32 H. P. Baltes, H. A. Ferwerda, A. S. Glass, B. Steinle: Opt. Acta **28**, 11 (1981)
8.33 J. C. Dainty, D. Newman: Opt. Lett. **8**, 608 (1983)
8.34 E. Jakeman, P. N. Pusey: J. Phys. A **8**, 369 (1975)
8.35 P. N. Pusey, E. Jakeman: J. Phys. A **8**, 392 (1975)
8.36 P. N. Pusey: In *Photon Correlation Spectroscopy and Velocimetry*, ed. by H. Z. Cummins, E. R. Pike (Plenum, New York 1977)
8.37 E. Jakeman: Proc. SPIE **243**, 9 (1980)
8.38 E. Jakeman, J. G. McWhirter: Appl. Phys. B **26**, 125 (1981)
8.39 E. Jakeman: In *Coherence and Quantum Optics* V, ed. by E. Wolf, L. Mandel (Plenum, New York 1984)
8.40 J. Uozumi, T. Asakura: J. Opt. **12**, 177 (1981)
8.41 Lord Rayleigh: Phil. Mag. **6**, 321 (1919)
8.42 J. Ohtsubo, T. Asakura: Opt. Commun. **25**, 315 (1978)
8.43 B. M. Levine, J. C. Dainty: Opt. Commun. **45**, 252 (1983)
8.44 E. Jakeman: J. Opt. Soc. Am. **72**, 1034 (1982)
8.45 M. Deka, S. P. Almeida, H. Fujii: J. Opt. Soc. Am. **71**, 155 (1981)
8.46 M. V. Berry: Adv. Phys. **25**, 1 (1976)
8.47 M. V. Berry, C. Upstill: *Progress in Optics* **15**, 605 (North-Holland, Amsterdam 1979)
8.48 J. G. Walker, M. V. Berry, C. Upstill: Opt. Acta **30**, 1001 (1983)
8.49 V. S. R. Guadimetla, J. F. Holmes: J. Opt. Soc. Am. **72**, 1213 (1982)
8.50 N. George, A. Jain: Opt. Commun. **15**, 71 (1975)
8.51 D. L. Fried: J. Opt. Soc. Am. **71**, 914 (1981)
8.52 K. A. O'Donnell: J. Opt. Soc. Am. **72**, 1459 (1982)
8.53 V. V. Anisimov, S. M. Kozel, G. R. Lokshin: Opt. Spectrosc. **27**, 258 (1969)
8.54 T. Asakura, N. Takai: Proc. SPIE **243**, 114 (1980)
8.55 T. Asakura, N. Takai: Appl. Phys. **25**, 179 (1981)
8.56 T. Iwai, N. Takai, T. Asakura: J. Opt. Soc. Am. **72**, 460 (1982)
8.57 K. A. O'Donnell: J. Opt. Soc. Am. **72**, 191 (1982)
8.58 L. Mandel: J. Opt. Soc. Am. **51**, 1342 (1961)
8.59 R. H. Boucher: J. Opt. Soc. Am. **71**, 1562 (1981)
8.60 N. George: Opt. Acta **23**, 36 (1976)

8.61 B. E. A. Saleh: Appl. Opt. **14**, 2344 (1975)
8.62 J. C. Erdmann, R. I. Gellert: J. Opt. Soc. Am. **66**, 1194 (1976)
8.63 N. Takai, T. Iwai, T. Asakura: Appl. Phys. B **26**, 185 (1981)
8.64 N. Takai, T. Iwai, T. Ushizaka, T. Asakura: J. Opt. **11**, 93 (1980)
8.65 J. Ohtsubo: Opt. Commun. **42**, 13 (1982)
8.66 A. E. Ennos: *Progress in Optics* **16**, 235 (North-Holland, Amsterdam 1978)
8.67 W. T. Welford: Opt. Quant. Electron. **9**, 269 (1977)
8.68 T. Asakura: In [8.4]
8.69 D. Legér, J. C. Perrin: J. Opt. Soc. Am. **66**, 1210 (1976)
8.70 J. Ohtsubo, T. Asakura: Optik **45**, 65 (1976)
8.71 H. Fujii, J. Uozumi, T. Asakura: J. Opt. Soc. Am. **66**, 1222 (1976)
8.72 J. Uozumi, H. Fujii, T. Asakura: J. Opt. Soc. Am. **67**, 808 (1977)
8.73 H. Fujii, T. Asakura: Opt. Commun. **21**, 80 (1977)
8.74 J. Ohtsubo: Appl. Opt. **21**, 4167 (1982)
8.75 Y. Y. Hung, C. Y. Liang: Appl. Opt. **18**, 1046 (1979)
8.76 D. A. Gregory: Opt. Laser Technol. **9**, 17 (1977)
8.77 A. E. Ennos, M. S. Virdee: Proc. IUTAM Conference on "Optical Methods in Mechanics of Solids", ed. by A. Lagarde (Sijthoff and Noordhoff, Amsterdam 1981) p. 331
8.78 A. E. Ennos: Opt. Commun. **33**, 9 (1980)
8.79 D. B. Barker, M. E. Fourney: Exp. Mech. **16**, 209 (1976)
8.80 F. P. Chiang: In *The Engineering Uses of Coherent Optics*, ed. by E. R. Robertson (University Press, Cambridge 1976) p. 209
8.81 T. D. Dudderar, P. G. Simkins: Nature **270**, 45 (1977)
8.82 K. A. Stetson: J. Opt. Soc. Am. **67**, 1587 (1977)
8.83 E. Archbold, A. E. Ennos, M. S. Virdee: Proc. SPIE **136**, 258 (1977)
8.84 K. A. Stetson: J. Opt. Soc. Am. **66**, 1267 (1976)
8.85 F. D. Adams, G. E. Maddux: US Air Force Tech. Memorandum AFFDL-TR-75-92 (1975)
8.86 G. B. Smith, K. A. Stetson: Appl. Opt. **19**, 3031 (1980)
8.87 P. M. Boone: Opt. Acta **22**, 579 (1975)
8.88 B. I. Ineichen, P. Eglin, R. Dandliker: Proc. ICO Conference, Madrid, ed. by J. Bescos, A. Hidalgo, L. Plaza, J. Santamaria (1978) p. 563
8.89 G. E. Maddux, S. L. Moorman, R. R. Corwin: US Air Force Tech. Report AFFDL-TM-78-109-FBE (1978)
8.90 G. F. Kaufman, A. E. Ennos, B. Gale, D. J. Pugh: J. Phys. E **13**, 579 (1980)
8.91 L. C. de Backer: Non-destructive Testing **8**, 17 (1975)
8.92 A. Happe: Proc. SPIE **136**, 270 (1977)
8.93 S. Ueha, N. Magone, J. Tsujiuchi: Opt. Commun. **27**, 324 (1978)
8.94 J. M. Burch, A. E. Ennos, G. B. Quinn: Israel J. Technol. **18**, 271 (1980)
8.95 J. M. Burch, C. Forno: Opt. Engrg. **14**, 178 (1975)
8.96 P. M. Boone, L. C. de Backer: Optik **44**, 343 (1976)
8.97 R. G. Hughes: In [8.88]
8.98 R. Jones, C. Wykes: Opt. Acta **28**, 949 (1981)
8.99 C. Wykes: Opt. Acta **24**, 517 (1977)
8.100 R. Jones, C. Wykes: Opt. Acta **24**, 533 (1977)
8.101 A. P. M. Hurden: Opt. Laser Technol. **14**, 21 (1982)
8.102 K. Hogmoen, O. J. Lokberg: Appl. Opt. **16**, 1869 (1977)
8.103 O. J. Lokberg, K. Hogmoen, O. H. Holge: Appl. Opt. **18**, 763 (1979)